

Search for the Blazhko effect in field RR Lyrae stars using LINEAR and ZTF light curves

Ema Donev¹ and Željko Ivezić²

¹ XV. Gymnasium (MIOC), Jordanovac 8, 10000, Zagreb, Croatia, e-mail: emadonev@icloud.com

² Department of Astronomy and the DiRAC Institute, University of Washington, 3910 15th Avenue NE, Seattle, WA, USA e-mail: ivezic@uw.edu

October 2024

ABSTRACT

We analyzed the incidence and properties of RR Lyrae stars that show evidence for amplitude and phase modulation (the so-called Blazhko Effect) in a sample of $\sim 3,000$ stars with LINEAR and ZTF light curve data. A preliminary subsample of about ~ 240 stars was algorithmically pre-selected using various data quality and light curve statistics, and then 139 stars were confirmed visually as displaying the Blazhko effect. This sample places a lower limit of 5% for the incidence of the Blazhko Effect in field RR Lyrae stars. Although close to 8,000 Blazhko stars were discovered or confirmed in the Galactic bulge and LMC/SMC by the OGLE-III survey, only about 200 stars have been reported in all field RR Lyrae stars studies to date; the sample presented here nearly doubles the number of field RR Lyrae stars displaying the Blazhko effect. With time-resolved photometry expected from LSST, a similar analysis will be performed for RR Lyrae stars in the southern sky and we anticipate a higher fraction of discovered Blazhko stars due to better sampling and superior photometric quality.

Key words. Variable stars — RR Lyrae stars — Blazhko Effect

1. Introduction

RR Lyrae stars are pulsating variable stars with periods in the range of 3–30 hours and large amplitudes that increase towards blue optical bands (e.g., in the SDSS g band from 0.2 mag to 1.5 mag; ?). For comprehensive reviews of RR Lyrae stars, we refer the reader to ? and ?.

RR Lyrae stars often exhibit amplitude and phase modulation, or the so-called Blazhko effect¹ (hereafter, “Blazhko stars”). For examples of well-sampled observed light curves showing the Blazhko effect, see, e.g., Kepler data shown in Figures 1 and 2 from ?. The Blazhko effect has been known for a long time (?), but its detailed observational properties and theoretical explanation of its causes remain elusive (??). Various proposed models for the Blazhko effect, and principal reasons why they fail to explain observations, are summarized in ?.

A part of the reason for the incomplete observational description of the Blazhko effect is difficulties in discovering a large number of Blazhko stars due to temporal baselines that are too short and insufficient number of observations per object (??). With the advent of modern sky surveys, several studies reported large increases in the number of known Blazhko stars, starting with a sample of about 700 Blazhko stars discovered by the MACHO survey towards the LMC (?) and about 500 Blazhko stars discovered by the OGLE-II survey towards the Galactic bulge (?). Most recently, about 4,000 Blazhko stars were discovered in the LMC and SMC (??), and an additional $\sim 3,500$ stars were discovered in the Galactic bulge (?), both by the OGLE-III survey. Nevertheless, discovering the Blazhko effect in field RR Lyrae stars that are spread over the entire sky remains a much harder

problem: only about 200 Blazhko stars in total from all the studies of field RR Lyrae stars have been reported so far (see Table 1 in ?).

Here, we report the results of a search for the Blazhko effect in a sample of $\sim 3,000$ field RR Lyrae stars with LINEAR and ZTF light curve data. A preliminary subsample of about ~ 240 stars was selected using various light curve statistics, and then ~ 140 stars were confirmed visually as displaying the Blazhko effect. This new sample greatly increases the number of known field RR Lyrae stars that exhibit the Blazhko effect. In §2 and §3 we describe our datasets and analysis methodology, and in §4 we present our analysis results. Our main results are summarized and discussed in §5.

2. Data Description and Period Estimation

Analysis of field RR Lyrae stars requires a sensitive time-domain photometric survey over a large sky area. For our starting sample, we used $\sim 3,000$ field RR Lyrae stars with light curves obtained by the LINEAR asteroid survey. In order to study long-term changes in light curves, we also utilized light curves obtained by the ZTF survey which monitored the sky ~ 15 years after LINEAR. The combination of LINEAR and ZTF provided a unique opportunity to systematically search for the Blazhko effect in a large number of field RR Lyrae stars.

We first describe each dataset in more detail, and then introduce our analysis methods. All our analysis code, written in Python, is available on GitHub².

¹ The Blazhko effect was discovered by Lidiya Petrovna Tseraskaya and first reported by Sergey Blazhko.

² https://github.com/emadonev/var_stars

57 **2.1. LINEAR Dataset**

58 The properties of the LINEAR asteroid survey and its photometric
 59 re-calibration based on SDSS data are discussed in ?. Briefly,
 60 the LINEAR survey covered about 10,000 deg² of the north-
 61 ern sky in white light (no filters were used, see Figure 1 in ?),
 62 with photometric errors ranging from ~0.03 mag at an equiva-
 63 lence SDSS magnitude of $r = 15$ to 0.20 mag at $r \sim 18$. Light
 64 curves used in this work include, on average, 270 data points
 65 collected between December 2002 and September 2008.

66 A sample of 7,010 periodic variable stars with $r < 17$ dis-
 67 covered in LINEAR data were robustly classified by ?, includ-
 68 ing about ~3,000 field RR Lyrae stars of both ab and c type,
 69 detected to distances of about 30 kpc (?). The sample used in
 70 this work contains 2196 ab-type and 745 c-type RR Lyrae,
 71 selected using classification labels and the gi color index from ?.
 72 The LINEAR light curves, augmented with IDs, equatorial coor-
 73 dinates, and other data, were accessed using the astroML Python
 74 module³ (?).

75 **2.2. ZTF Dataset**

76 The Zwicky Transient Factory (ZTF) is an optical time-domain
 77 survey that uses the Palomar 48-inch Schmidt telescope and a
 78 camera with 47 deg² field of view (?). The dataset analyzed here
 79 was obtained with SDSS-like g , r , and i band filters. Light curves
 80 for objects in common with the LINEAR RR Lyrae sample typ-
 81 ically have smaller random photometric errors than LINEAR
 82 light curves because ZTF data are deeper (compared to LINEAR,
 83 ZTF data have about 2-3 magnitudes fainter 5 σ depth). ZTF data
 84 used in this work were collected between February 2018 and De-
 85 cember 2023, on average about 15 years after obtaining LINEAR
 86 data.

87 The ZTF dataset for this project was created by selecting
 88 ZTF IDs with matching equatorial coordinates to a correspond-
 89 ing LINEAR ID of an RR Lyrae star. This process used the
 90 `ztfquery` function, which searched the coordinates in the ZTF
 91 database within 3 arcsec from the LINEAR position. The result-
 92 ing sample consisted of 2857 RR Lyrae stars with both LINEAR
 93 and ZTF data. The fractions of RRab and RRc type RR Lyrae in
 94 this sample, 71% RRab and 29% RRc type, are consistent with
 95 results from other surveys (e.g., ?).

96 **2.3. Period Estimation**

97 The first step of our analysis is estimating best-fit periods, sepa-
 98 rately for LINEAR and ZTF datasets. We used the Lomb-Scargle
 99 method (?) as implemented in `astropy` (?). The period estima-
 100 tion used 3 Fourier components and a two-step process: an ini-
 101 tial best-fit frequency was determined using the `autopower` fre-
 102 quency grid option and then the power spectrum was recom-
 103 puted around the initial frequency using an order of magnitude
 104 smaller frequency step. In case of ZTF, we estimated period
 105 separately for each available passband and adopted their mean
 106 value. Once the best-fit period was determined, a best-fit model
 107 for the phased light curve was computed using 6 Fourier compo-
 108 nents. Fig 1 shows an example of a star with LINEAR and ZTF
 109 light curves, phased light curves, and their best-fit models.

110 We found excellent agreement between the best-fit periods
 111 estimated separately from LINEAR and ZTF light curves. The
 112 median of their ratio is unity within 2×10^{-6} and the robust stan-

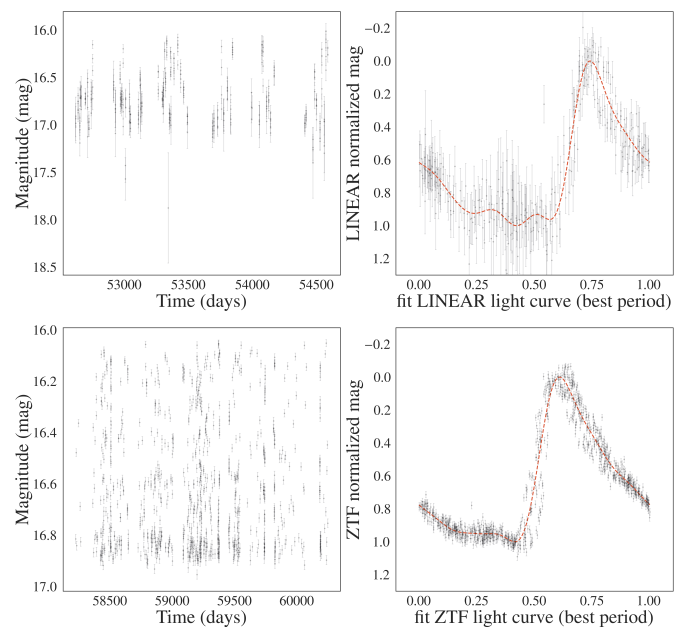


Fig. 1. An example of a (Blazhko?) star with LINEAR (top row) and ZTF (bottom row) light curves (left panels, data points with “error bars”), phased light curves normalized to the 0–1 range (right panels, data points with “error bars”), with their best-fit models shown by dashed lines.

dard deviation of their ratio is 2×10^{-5} . With a median sample period of 0.56 days, the implied scatter of period difference is about 1.0 sec.

Given on average about 15 years between LINEAR and ZTF data sets, and a typical period of 0.56 days, this time difference corresponds to about 10,000 oscillations. With a fractional period uncertainty of 2×10^{-5} , LINEAR data can predict the phase of ZTF light curve with an uncertainty of 0.2. Therefore, for a robust detection of light curve phase modulation, each data set must be analyzed separately. On the other hand, amplitude modulation can be detected on time scales as long as 15 years, as discussed in the following section.

3. Analysis Methodology: Searching for the Blazhko Effect

Given the two sets of light curves from LINEAR and ZTF, we searched for amplitude and phase modulation, either during the 5–6 years of data taking by each survey, or during the average span of 15 years between the two surveys. Starting with a sample of 2857 RR Lyrae stars, we pre-selected a smaller sample that was inspected visually (see below for details). We also required at least 250 LINEAR data points and 40 ZTF data points (per band) in analyzed light curves. We used two pre-selection methods that are sensitive to different types of light curve modulation: direct light curve analysis and periodogram analysis, as follows.

3.1. Direct Light Curve Analysis

Given statistically correct period, amplitude and light curve shape estimates, as well as data being consistent with reported (presumably Gaussian) uncertainty estimates, the χ^2 per degree of freedom gives a quantitative assessment of the “goodness of

³ For an example of light curves, see https://www.astroml.org/book_figures/chapter10/fig_LINEAR_LS.html

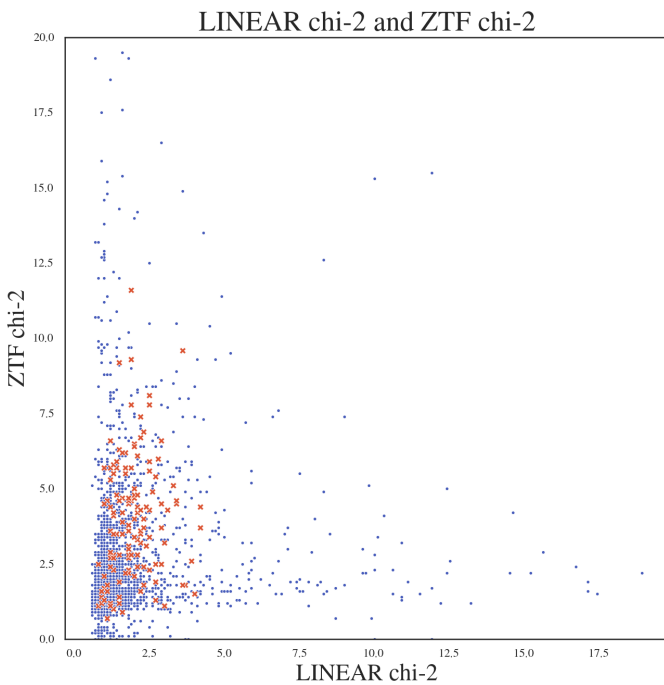


Fig. 2. A diagram constructed with the two sets of χ^2_{dof} values, for LINEAR and ZTF data sets, where blue symbols represents all RR Lyrae stars and the red symbols are the final sample of Blazhko stars.

143 fit",

$$\chi^2_{dof} = \frac{1}{N_{dof}} \sum \frac{(d_i - m_i)^2}{\sigma_i^2}. \quad (1)$$

144 Here, d_i are measured light curve data values at times t_i , and with
145 associated uncertainties σ_i , m_i are best-fit models at times t_i , and
146 N_{dof} is the number of degrees of freedom, essentially the num-
147 ber of data points. In the absence of any light curve modulation,
148 the expected value of χ^2_{dof} is unity, with a standard deviation
149 of $\sqrt{2}/N_{dof}$. If $\chi^2_{dof} - 1$ is many times larger than $\sqrt{2}/N_{dof}$,
150 it is unlikely that data d_i were generated by the assumed (un-
151 changing) model m_i . Of course, χ^2_{dof} can also be large due to
152 underestimated measurement uncertainties σ_i , or to occasional
153 non-Gaussian measurement error (the so-called outliers).

154 Therefore, to search for signatures of the Blazhko effect,
155 manifested through statistically unlikely large values of χ^2_{dof} , we
156 computed χ^2_{dof} separately for LINEAR and ZTF data (see Figure
157 2). Using the two sets of χ^2_{dof} values, we algorithmically pre-
158 selected a sample of candidate Blazhko stars for further visual
159 analysis of their light curves. The visual analysis is needed to
160 confirm the expected Blazhko behavior in observed light curves,
161 as well as to identify cases of data problems, such as photometric
162 outliers.

163 We used a simple scoring algorithm, optimized through trial
164 and error, such that for LINEAR the range $1.8 < \chi^2_{dof} < 3.0$
165 was worth 2 points and $\chi^2_{dof} > 3.0$ worth 3 points, while for
166 ZTF $2.0 < \chi^2_{dof} < 4.0$ and $\chi^2 > 4.0$ were the analogous limits.
167 In addition, we also considered normalized period differences
168 (dP) and amplitude differences (dA) and assigned: 2 points for
169 $0.00002 < dP < 0.00005$ and 4 points for $dP > 0.00005$; 1 point
170 for $0.05 < dA < 0.15$ and 2 points for $dA > 0.15$. A star could
171 score a maximum of 12 points, and a minimum of 5 points was
172 required for further visual analysis.

The sample pre-selected using this method includes 189
173 stars. For most selected stars, the χ^2_{dof} values were larger for the
174 ZTF data because the ZTF photometric uncertainties are smaller
175 than for the LINEAR data set. Fig. 3 summarizes the selection
176 criteria and the resulting numbers of selected stars for each cri-
177 terion and their combinations.

3.2. Periodogram Analysis

When light curve modulation is due to double-mode oscillation
180 with two similar oscillation frequencies (periods), it is possible
181 to recognize its signature in the periodogram computed as part of
182 the Lomb-Scargle analysis. Depending on various details, such
183 as data sampling and the exact values of periods, amplitudes, this
184 method may be more efficient than direct light curve analysis.

A sum of two *sine* functions with same amplitudes and with
185 frequencies f_1 and f_2 can be rewritten using trigonometric equa-
186 tions as

$$y(t) = 2 \cos(2\pi \frac{f_1 - f_2}{2} t) \sin(2\pi \frac{f_1 + f_2}{2} t). \quad (2)$$

We can define

$$f_o = \frac{f_1 + f_2}{2}, \quad (3)$$

and

$$\Delta f = |\frac{f_1 - f_2}{2}|, \quad (4)$$

with $\Delta f \ll f_o$ when f_1 and f_2 are similar. The fact that Δf is
191 much smaller than f_o means that the period of the *cos* term is
192 much larger than the period of the basic oscillation (f_o). In other
193 words, the *cos* term acts as a slow amplitude modulation of the
194 basic oscillation. When the amplitudes of two *sine* functions are
195 not equal, the results are more complicated but the basic con-
196 clusion about amplitude modulation remains. When the power
197 spectrum of $y(t)$ is constructed, it will show 3 peaks: the main
198 peak at f_o and two more peaks at frequencies $f_o \pm \Delta f$. We used
199 this fact to construct an algorithm for automated searching for
200 the evidence of amplitude modulation. Fig 4 compares the theo-
201 retical periodogram produced by interference beats with our al-
202 gorithm's periodogram, signifying that local Blazhko peaks are
203 present in real data.

204 After the strongest peak in the Lomb-Scargle periodogram
205 is found at frequency f_o , we search for two equally distant local
206 peaks at frequencies f_- and f_+ , with $f_- < f_o < f_+$. The sideband
207 peaks can be highly asymmetric ? and observed peri-
208 odograms can sometimes be much more complex ?. We fold
209 the periodogram through the main peak at f_o , multiply the two
210 branches and then search for the strongest peaks in the result-
211 ing folded periodogram that is statistically more significant than
212 the background noise. The background noise is computed as the
213 scatter of the folded periodogram estimated from the interquar-
214 tile range. We require a “signal-to-noise” ratio of at least 5, as
215 well as the peak strength of at least 0.05. If such a peak is found,
216 and it doesn't correspond to yearly alias, we select the star as a
217 candidate Blazhko star and compute its Blazhko period as

$$P_{BL} = |f_{-,+} - f_o|^{-1},$$

218 where $f_{-,+}$ means the Blazhko sideband frequency with a higher
219 amplitude is chosen.

220 The observed Blazhko periods range from 3 to 3,000 days,
221 and Blazhko amplitudes range from 0.01 mag to about 0.3 mag

Analysis of blazhko star metrics for RR Lyrae

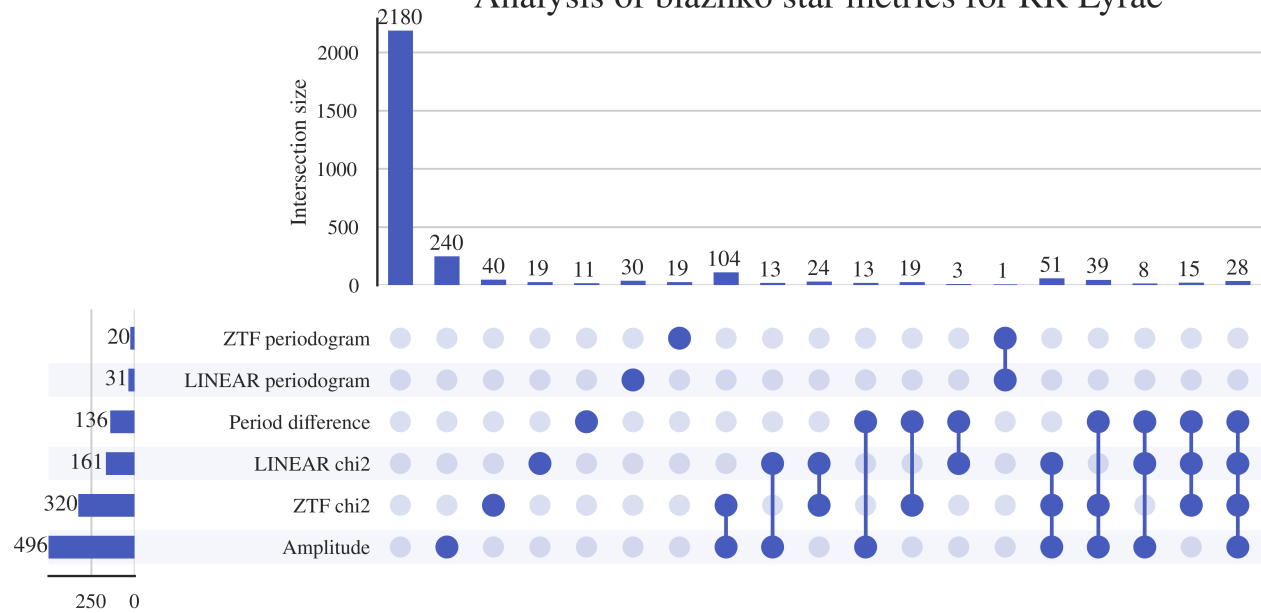


Fig. 3. The figure shows selection criteria and the resulting numbers of pre-selected Blazhko star candidates for each criterion and their combinations. The dots represent each case a star can occupy, where every solid dot is a specific criterion that is satisfied. Connections between solid dots represent stars which satisfy multiple criteria. Each dot combination has its own count, represented by the horizontal countplot. The vertical countplot shows the total number of stars that satisfy one criteria (union of all cases).

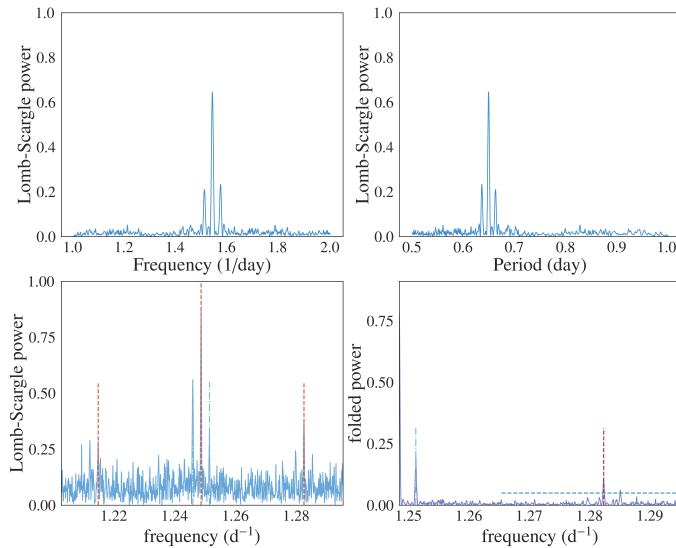


Fig. 4. The top two panels show a simulated periodogram for a sum of two \sin functions with similar frequencies – the central peak corresponds to their mean. The bottom left panel shows a periodogram for an observed LINEAR light curve, and the bottom right panel shows its folded version. The vertical dashed lines show the three frequencies identified by the algorithm described in text.

3.2.1. Visual Confirmation

The sample pre-selected for visual analysis includes 239 RR Lyrae stars ($189 + 51$, with one star selected twice), or 8.4% of the starting LINEAR-ZTF sample. Visual analysis included the following standard steps (e.g., ?):

1. The shape of the phased light curves and scatter of data points around the best-fit model were examined for signatures of anomalous behavior indicative of the Blazhko effect. Fig. 6 shows an example of such behavior where the ZTF data and fit show multiple coherent data point sequences offset from the best-fit mean model.
2. Full light curves were inspected for their repeatability between observing seasons (Fig. 7). This step was sensitive to amplitude modulations with periods of the order a year or longer.
3. The phased light curves normalized to unit amplitude were inspected for their repeatability between observing seasons. This step was sensitive to phase modulations of a few percent or larger on time scales of the order a year or longer. Fig. 8 shows an example of a Blazhko star where season-to-season phase (and amplitude) modulations are seen in both the LINEAR data and (especially) the ZTF data.

After visually analyzing the starting sample of 239 Blazhko candidates, we visually confirmed expected Blazhko behavior for 136 stars (112 out of 189 and 24 out of 50). LINEAR IDs and other characteristics for confirmed Blazhko stars are listed in Table 1 (Appendix A). Statistical properties of the selected sample of Blazhko stars are discussed in detail in the next section.

STOPPED HERE

4. Results

UNFINISHED

(?). In this work, we selected a smaller Blazhko range due to the limitations of our data: 30–325 days. With this additional constraint, we selected 51 candidate Blazhko stars, with one star already included in the sample of 189 stars described in preceding section. Fig 5 shows an example where two very prominent peaks were identified in the LINEAR periodogram.

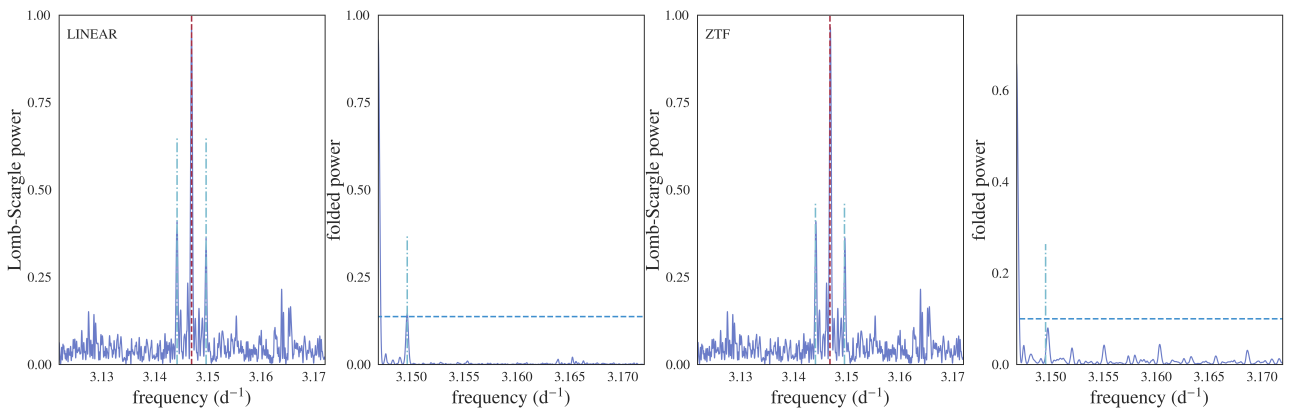


Fig. 5. Phase 2 of visual analysis of Blazhko candidates. XXX Are these LINEAR and ZTF periodograms? Is this figure a bit redundant with the previous figure?

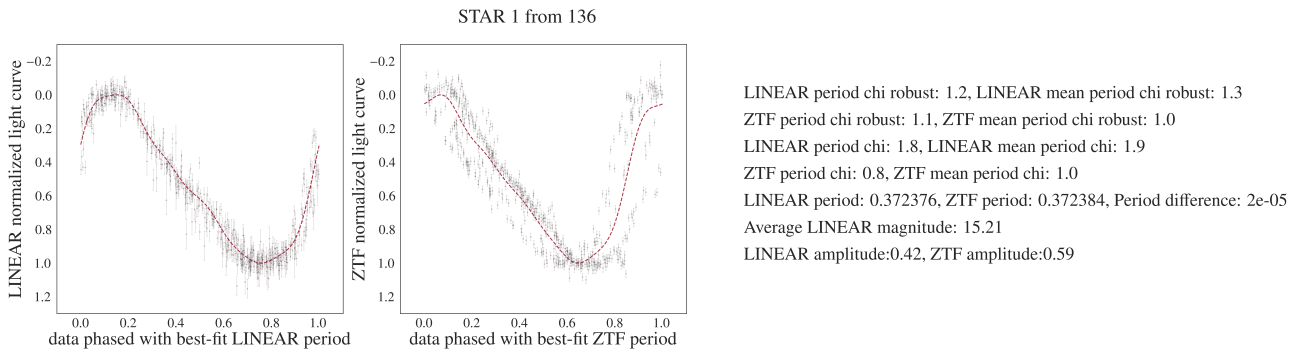


Fig. 6. An illustration of visual analysis of phased light curves for the selected Blazhko candidates. The left panel shows LINEAR data and the right panel shows ZTF data (symbols with “error bars”). The dashed lines are best-fit models. The numbers listed on the right side were added to aid visual analysis. Note multiple coherent data point sequences offset from the best-fit mean model in the right panel.

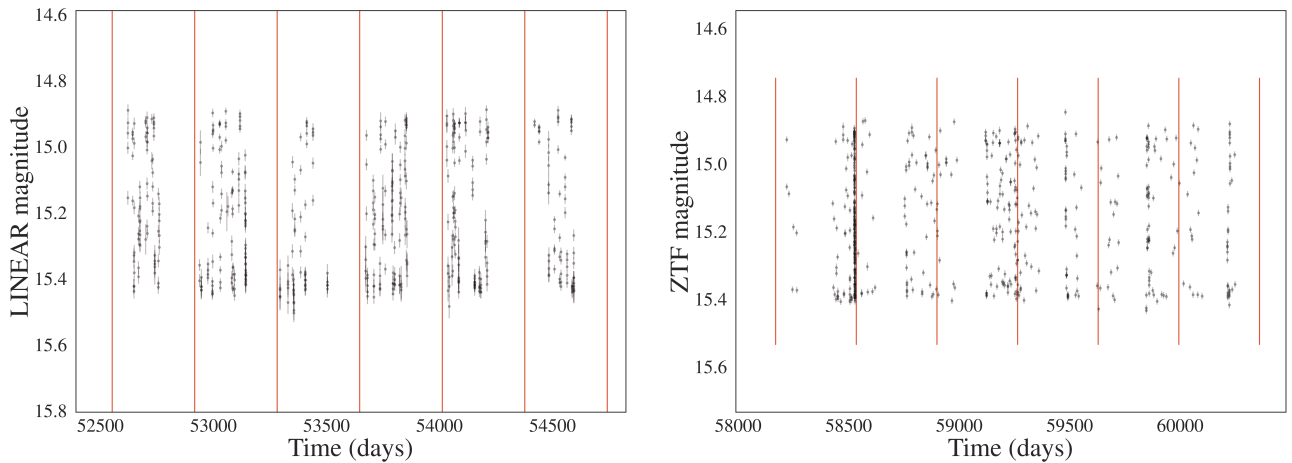


Fig. 7. Visual analysis of full light curves for the selected Blazhko candidates with emphasis on their repeatability between observing seasons, marked with vertical lines (left: LINEAR data; right: ZTF data).

Starting with a sample of 2857 field RR Lyrae stars with both LINEAR and ZTF data, we found 136 stars exhibiting convincing Blazhko effect. In Appendix A, the reader can find all of the Blazhko stars and some elementary data describing each star.

Another important note highlighting the difficulty of finding Blazhko stars is that the absolute Blazhko frequency difference from the main frequency is approximately 0.028 d^{-1} . Also, the average period difference between LINEAR and ZTF in Blazhko stars was around 0.0001 days. These minimal differences require precise observations over a long temporal baseline.

Finally, we have discovered that in some Blazhko stars, the effect cannot be detected ten years later or beforehand. When comparing LINEAR and ZTF data, some pairs have the effect present in only one dataset and others in both. This finding could mean that the Blazhko effect is not always present and gives us a clue about its mechanism. However, the precision of data is also a factor for consideration.

Seasons for:7048826

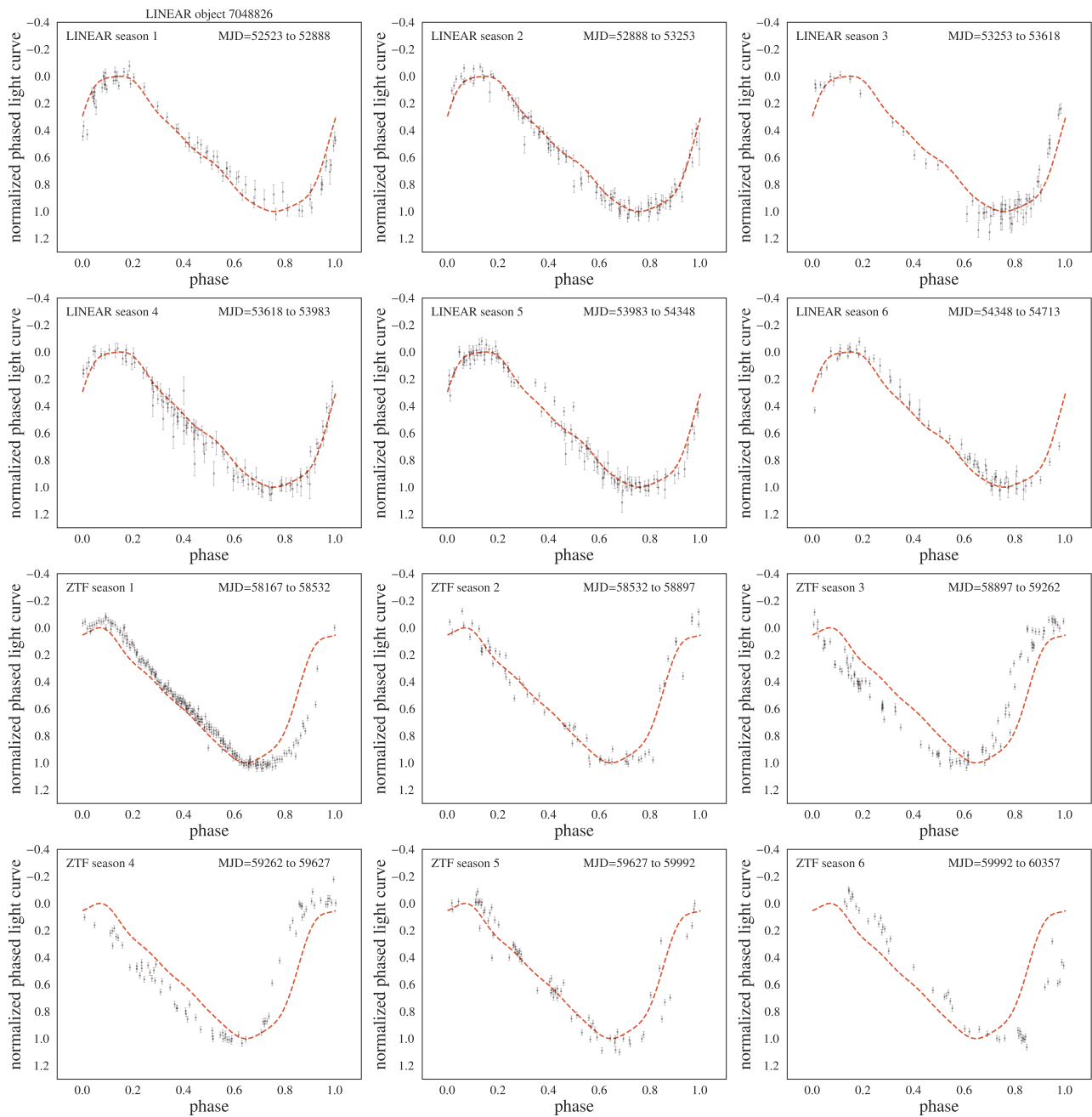


Fig. 8. The phased light curves normalized to unit amplitude are shown for single observing seasons and compared to the mean best-fit models (top six panels: LINEAR data; bottom six panels: ZTF data). Season-to-season phase and amplitude modulations are seen in both the LINEAR and the ZTF data.

279 5. Discussion and Conclusions

280 UNFINISHED

281 The reported incidence rates for the Blazhko effect range
 282 from 5% (?) to 60% (?). For a relatively small sample of 151
 283 stars with Kepler data, a claim has been made that essentially
 284 every RR Lyrae star exhibits modulated light curve (?). The dif-
 285 ference in Blazhko incidence rates for the two most extensive
 286 samples, obtained by the OGLE-III survey for the Large Magel-
 287 lanic Cloud (LMC, 20% out of 17,693 stars; ?). Moreover, the
 288 Galactic bulge (30% out of 11,756 stars; ?) indicates a possible
 289 variation of the Blazhko incidence rate with underlying stellar

290 population properties. In this work, 4.67% of the original RR
 291 Lyrae dataset are Blazhko stars. Since our sample size is consider-
 292 able, we conclude that the incidence rate of Blazhko stars in
 293 our work is representative and aligns with other works. We the-
 294 orize that the difference in incidence rates occurs due to varying
 295 data precision, the temporal baseline length, and differences in
 296 visual or algorithmic analysis. We also conclude that our algo-
 297 rithm's success rate in finding 136 out of 239 potential Blazhko
 298 stars is 57%. This high number indicates that the algorithm is
 299 very successful and can be used and refined further for efficient
 300 Blazhko star selection.

For future research, we would like to explore the final finding and find a connection or a factor that might give rise to a mechanism that explains the Blazhko effect. The project is an excellent example of automatizing the search for Blazhko stars. It can further be improved by training a neural network to replace visual analysis, and our current algorithms can be improved with other models. This work can provide a base for finding more Blazhko stars for the future Vera Rubin observatory. The Legacy Survey of Space and Time (LSST; ?) will be an excellent survey for studying Blazhko effect (?) because it will have both a long temporal baseline (10 years) and a large number of observations per object (nominally 825; LSST Science Requirements Document⁴).

Claim from the abstract: With time-resolved photometry expected from LSST, a similar analysis will be performed for RR Lyrae stars in the southern sky and we anticipate a higher fraction of discovered Blazhko stars due to better sampling and superior photometric quality. Support with this quote:

the incidence rate of the Blazhko effect increases with sensitivity to small-amplitude modulation, and thus with photometric data quality (?).

We confirm that the light curve modulation can be unstable, as discussed by ?

From ?: A sample of 30 RRab stars was extensively observed, and light-curve modulation was detected in 14 cases. The 47 per cent occurrence rate of the modulation is much larger than any previous estimate.

Acknowledgements. We thank Mathew Graham for providing *ztfquery* code example to us. Ž.I. acknowledges funding by the Fulbright Foundation and thanks the Ruđer Bošković Institute (Zagreb, Croatia) for hospitality. Based on observations obtained with the Samuel Oschin Telescope 48-inch and the 60-inch Telescope at the Palomar Observatory as part of the Zwicky Transient Facility project. ZTF is supported by the National Science Foundation under Grants No. AST-1440341 and AST-2034437 and a collaboration including current partners Caltech, IPAC, the Weizmann Institute of Science, the Oskar Klein Center at Stockholm University, the University of Maryland, Deutsches Elektronen-Synchrotron and Humboldt University, the TANGO Consortium of Taiwan, the University of Wisconsin at Milwaukee, Trinity College Dublin, Lawrence Livermore National Laboratories, IN2P3, University of Warwick, Ruhr University Bochum, Northwestern University and former partners the University of Washington, Los Alamos National Laboratories, and Lawrence Berkeley National Laboratories. Operations are conducted by COO, IPAC, and UW. The LINEAR program is funded by the National Aeronautics and Space Administration at MIT Lincoln Laboratory under Air Force Contract FA8721-05-C-0002. Opinions, interpretations, conclusions and recommendations are those of the authors and are not necessarily endorsed by the United States Government.

References

Alcock, C., Alves, D. R., Becker, A., et al. 2003, ApJ, 598, 597	348
Astropy Collaboration, Price-Whelan, A. M., Sipőcz, B. M., et al. 2018, AJ, 156, 123	349
Bellm, E. C., Kulkarni, S. R., Graham, M. J., et al. 2019, PASP, 131, 018002	350
Benkő, J. M., Kolenberg, K., Szabó, R., et al. 2010, MNRAS, 409, 1585	351
Blažko, S. 1907, Astronomische Nachrichten, 175, 325	352
Catelan, M. 2009, Ap&SS, 320, 261	353
Hernitschek, N. & Stassun, K. G. 2022, ApJS, 258, 4	354
Ivezić, Ž., Kahn, S. M., Tyson, J. A., et al. 2019, ApJ, 873, 111	355
Jurcsik, J., Sódor, Á., Szeidl, B., et al. 2009, MNRAS, 400, 1006	356
Kolenberg, K. 2008, in Journal of Physics Conference Series, Vol. 118, Journal of Physics Conference Series (IOP), 012060	357
Kovács, G. 2009, in American Institute of Physics Conference Series, Vol. 1170, Stellar Pulsation: Challenges for Theory and Observation, ed. J. A. Guzik & P. A. Bradley, 261–272	358
Kovács, G. 2016, Communications of the Konkoly Observatory Hungary, 105, 61	359
Kovács, G. 2018, A&A, 614, L4	360
Mizerski, T. 2003, Acta Astron., 53, 307	361
Palaversa, L., Ivezić, Ž., Eyer, L., et al. 2013, AJ, 146, 101	362
Sesar, B., Ivezić, Ž., Grammer, S. H., et al. 2010, ApJ, 708, 717	363
Sesar, B., Ivezić, Ž., Stuart, J. S., et al. 2013, AJ, 146, 21	364
Sesar, B., Stuart, J. S., Ivezić, Ž., et al. 2011, AJ, 142, 190	365
Smith, H. A. 1995, Cambridge Astrophysics Series, 27	366
Soszyński, I., Dziembowski, W. A., Udalski, A., et al. 2011, Acta Astron., 61, 1	367
Soszyński, I., Udalski, A., Szymański, M. K., et al. 2010, Acta Astron., 60, 165	368
Soszyński, I., Udalski, A., Szymański, M. K., et al. 2009, Acta Astron., 59, 1	369
Szabó, R. 2014, in IAU Symposium, Vol. 301, Precision Asteroseismology, ed. J. A. Guzik, W. J. Chaplin, G. Handler, & A. Pigulski, 241–248	370
Szabó, R., Benkő, J. M., Paparó, M., et al. 2014, A&A, 570, A100	371
Szczygieł, D. M. & Fabrycky, D. C. 2007, MNRAS, 377, 1263	372
Vanderplas, J. 2015, gatspy: General tools for Astronomical Time Series in Python	373
VanderPlas, J., Connolly, A. J., Ivezić, Z., & Gray, A. 2012, in Proceedings of Conference on Intelligent Data Understanding (CIDU), 47–54	374

⁴ Available as ls.st/srd

Appendix A: Full table of results

Here we present all the confirmed Blazhko stars with their LINEAR IDs, equatorial coordinates, and calculated periods and χ^2 values.

LINEAR ID	RA	DEC	LINEAR period	ZTF period	LINEAR chi-2	ZTF chi-2
523832	207.529404	33.706001	0.372376	0.372384	1.20	1.10
1240665	206.202469	34.058662	0.632528	0.632522	3.00	1.10
1736308	206.096115	36.648674	0.555848	0.555843	1.30	1.00
2669011	206.229523	38.758453	0.591153	0.591151	1.10	0.70
2742032	207.355225	39.589951	0.629676	0.629692	0.90	1.40
2812086	206.805511	40.859066	0.646015	0.646000	3.00	3.20
3507643	206.557358	39.536449	0.801141	0.801132	1.60	0.90
5931160	207.177231	41.918797	0.664700	0.664708	0.80	1.10
6665721	206.020233	41.646141	0.643318	0.643325	1.00	1.70
17185566	206.387268	43.314617	0.614160	0.614169	1.50	1.90
22828215	206.657028	43.543236	0.574536	0.574535	1.50	1.40
29848	206.917358	44.971054	0.557020	0.557040	1.40	3.50
158779	207.772202	45.916824	0.609207	0.609189	1.60	3.90
263541	207.172470	45.713154	0.558218	0.558221	2.90	6.60
514883	206.594757	46.482040	0.557723	0.557737	1.70	5.50
737951	206.435547	45.881615	0.357023	0.357023	2.20	6.70
810169	169.297485	6.265203	0.465185	0.465212	2.10	2.80
924301	169.713531	6.963072	0.507503	0.507440	1.90	9.30
1092244	207.060974	5.649392	0.649496	0.649558	1.20	3.60
1244554	206.944962	5.346962	0.536875	0.536962	1.80	2.30
1307948	206.223587	6.741248	0.527474	0.527415	1.80	4.50
1332201	207.992432	-4.603579	0.580711	0.580731	1.60	4.20
1390653	207.220245	-3.214271	0.521867	0.521871	1.30	4.10
1435279	207.824600	-3.712567	0.381858	0.381860	2.10	4.20
1448299	206.582916	51.406654	0.606912	0.606940	2.70	5.40
1593736	169.096771	5.428976	0.592628	0.592650	1.20	5.70
1748058	207.353790	53.020401	0.310237	0.310176	1.40	5.70
1857382	206.026001	56.421604	0.566428	0.566407	2.70	2.50
1882354	207.117645	56.313797	0.695061	0.695029	1.50	2.80
2041979	206.848053	55.248009	0.653694	0.653639	1.20	5.30
2075949	207.733643	62.320267	0.477806	0.477666	1.60	4.70
2117028	207.188278	61.978554	0.591245	0.591243	2.20	3.50
2122319	206.210190	62.778843	0.359422	0.359424	2.10	6.10
2229607	207.042603	65.877083	0.575179	0.575211	1.20	4.40
2243683	206.780823	8.893113	0.579777	0.579803	3.10	4.30
2248787	206.407776	7.914382	0.563528	0.563539	2.10	2.40
2334384	206.454544	7.380644	0.555341	0.555333	2.00	6.50
2397296	168.680649	51.998081	0.488814	0.488836	1.20	6.60
2414841	206.101624	7.666218	0.559611	0.559592	1.70	5.70
2455568	168.211075	51.534416	0.594119	0.594092	2.00	2.10
2612592	207.693237	-5.975360	0.571562	0.571543	1.30	2.80
2653982	168.135025	51.014339	0.607082	0.607110	1.00	2.10
2766997	207.782440	-7.099904	0.289881	0.289943	1.80	3.60
2892940	209.495773	2.587467	0.539855	0.539896	1.30	4.20
3036295	209.338211	2.393512	0.629705	0.629714	1.80	2.20
3140139	208.758163	-0.100046	0.304590	0.304585	2.50	5.60
3183285	208.391159	0.479103	0.349653	0.349664	1.20	2.80
3196582	208.521881	0.740297	0.268017	0.268018	2.50	3.40
3196780	169.384384	53.303658	0.504148	0.504199	2.20	3.20
3294319	169.550766	53.459976	0.555460	0.555473	1.90	4.70
3437725	208.845749	12.514306	0.542457	0.542478	1.50	6.30
3591037	208.146072	14.167974	0.558643	0.558609	1.30	3.50
3941776	209.073120	13.401526	0.532222	0.532209	2.80	6.00
4101289	209.351425	13.537904	0.379225	0.379250	1.20	2.70
4586691	208.326218	15.475822	0.621459	0.621446	2.00	3.40
4804945	209.674210	16.421736	0.556172	0.556217	2.50	7.80
5421989	208.014435	18.561077	0.534510	0.534527	0.80	2.50

LINEAR ID	RA	DEC	LINEAR period	ZTF period	LINEAR chi-2	ZTF chi-2
6582265	209.421219	17.441139	0.691751	0.691749	2.90	3.70
6651516	208.909760	17.881287	0.308488	0.308496	1.30	5.80
6819457	209.491974	20.296762	0.436282	0.436265	3.60	9.60
6883239	208.333481	19.276327	0.563711	0.563712	2.90	2.50
6967017	208.406662	21.846382	0.529691	0.529677	2.30	6.90
7048826	208.492981	22.591896	0.317781	0.317790	1.40	5.90
7254801	209.648148	22.561989	0.561133	0.561071	1.30	5.50
7279621	208.915436	24.833937	0.415469	0.415467	1.90	4.60
7283275	208.409698	26.350325	0.543342	0.543331	2.20	3.60
7344401	209.188583	26.111385	0.330201	0.330226	1.80	2.70
7580734	209.349243	26.322409	0.314956	0.314957	2.00	4.00
7657340	208.098282	27.700201	0.495480	0.495493	2.30	4.00
7811366	208.457687	30.868412	0.489523	0.489521	2.00	4.70
7827663	208.047531	30.799057	0.390832	0.390832	3.40	4.50
7846640	209.106400	4.330462	0.551495	0.551518	1.50	9.20
8222011	209.258850	3.100914	0.350920	0.350914	2.00	4.80
8311517	208.212936	4.452833	0.523354	0.523359	1.80	3.60
8331094	208.446945	3.969552	0.267543	0.267549	2.10	3.30
8343291	208.919601	-2.689821	0.569785	0.569791	3.30	5.10
9063194	169.357468	57.331566	0.575781	0.575760	2.40	3.10
9236215	209.009872	-1.607280	0.352570	0.352572	1.80	2.80
9449335	209.488937	-2.928472	0.475720	0.475695	2.00	5.00
9532981	168.695602	60.104759	0.591000	0.591042	1.70	6.20
9918809	209.255295	-2.089725	0.479460	0.479509	1.90	11.60
9968431	209.717804	-2.437493	0.302266	0.302211	1.70	2.20
9979905	208.905365	31.572962	0.338739	0.338739	2.50	2.30
10030349	209.547668	32.537975	0.545073	0.545074	2.10	4.40
10260828	208.891602	32.249817	0.380655	0.380643	2.20	7.40
10814742	209.570526	31.039347	0.462687	0.462683	2.50	4.30
11215595	208.180191	33.574619	0.546960	0.546943	1.30	2.30
16991760	209.105652	33.977589	0.549098	0.549096	2.90	3.70
17247918	169.489120	59.391106	0.481867	0.481865	1.80	4.60
17275627	208.806717	33.957424	0.537775	0.537771	2.10	4.80
17302403	209.807205	35.285717	0.488261	0.488343	2.00	6.40
17544856	208.748581	36.859768	0.614297	0.614296	2.00	3.40
19775800	208.958618	36.484657	0.310856	0.310867	1.30	2.70
21488669	209.334930	37.248749	0.501644	0.501661	1.90	5.70
21556651	208.269577	38.000725	0.614826	0.614808	1.80	3.10
21619184	208.125366	37.095997	0.557343	0.557320	2.30	3.70
21806402	208.151657	39.543987	0.592081	0.592104	1.60	6.20
21874209	209.602371	40.245346	0.611295	0.611286	2.50	5.90
21967825	209.202347	39.452202	0.540607	0.540600	1.80	4.70
22244513	208.742203	41.386112	0.604149	0.604077	2.50	8.10
22319996	209.734711	42.773571	0.479505	0.479495	2.60	4.90
22518636	208.239105	41.299026	0.283996	0.283998	1.80	3.00
22959674	209.018127	41.835575	0.405333	0.405409	1.80	3.80
22980793	208.105713	44.400867	0.540348	0.540353	1.90	2.80
23135759	209.604721	45.746510	0.402730	0.402732	4.20	4.40
23148883	209.446594	45.757584	0.390130	0.390124	1.40	4.80
23184808	208.547745	47.825001	0.338821	0.338888	1.00	5.70
23193507	208.703445	49.226929	0.473158	0.473174	3.40	4.60
23653629	209.116013	50.653641	0.442052	0.442055	2.40	4.40
24019356	208.649506	50.454273	0.517473	0.517460	1.50	4.60
24020106	209.853088	5.836339	0.542397	0.542396	2.90	4.50
24216004	209.385406	6.251467	0.382077	0.381912	1.90	7.80
880588	208.532242	6.762656	0.600138	0.600134	1.20	2.40
1212611	208.592422	6.144436	0.630896	0.630893	0.90	1.20
1876491	209.131027	5.983884	0.760128	0.760123	1.20	1.20
3048546	209.125137	-4.194337	0.656287	0.656293	1.00	1.30
5272753	208.115189	-4.847239	0.485827	0.485831	0.90	1.60
8610884	208.744736	-4.852155	0.592421	0.592429	2.20	4.30
8907563	209.521454	-3.322183	0.513164	0.513164	1.10	4.60

LINEAR ID	RA	DEC	LINEAR period	ZTF period	LINEAR chi-2	ZTF chi-2
9852554	208.390961	-4.619442	0.651339	0.651367	1.00	4.50
9961135	209.178848	52.903030	0.590896	0.590891	1.10	1.80
10503746	208.417831	54.266953	0.573563	0.573570	2.70	1.90
21948290	209.862518	56.455978	0.511127	0.511115	2.30	2.40
23596342	209.988663	56.828396	0.602841	0.602846	1.20	2.90
23898397	121.150764	42.483574	0.563018	0.562989	1.60	3.50
1882088	208.323578	58.245502	0.315984	0.316041	4.00	1.50
2936953	208.351578	57.226521	0.328746	0.328733	2.70	1.30
3219035	209.858856	60.601982	0.326746	0.326509	3.90	2.60
4320492	168.062149	65.801857	0.361005	0.360942	3.70	1.80
8036191	208.732498	59.448402	0.363860	0.363893	2.20	1.60
10420063	209.945786	61.264187	0.487395	0.487394	4.20	3.70
10662468	209.124405	61.076996	0.445180	0.445167	3.60	1.80
21688272	209.311371	62.800976	0.304803	0.304790	2.30	1.80
2714034	168.354202	65.678604	0.610868	0.610800	1.50	1.20
5592590	208.440872	65.857277	0.346945	0.346980	1.20	1.10
8799313	208.821136	7.846983	0.327560	0.327542	1.10	1.60